Mechanics of Materials 140 (2020) 103228

Contents lists available at ScienceDirect

Mechanics of Materials

journal homepage: www.elsevier.com/locate/mechmat

Research paper

A micromechanics-based constitutive model for linear viscoelastic particle-reinforced composites

Yang Chen[a], Pingping Yang[b], Yexin Zhou[c], Zaoyang Guo[c,*], Leiting Dong[a,*], Esteban P. Busso[c]

[a] School of Aeronautic Science and Engineering, Beihang University, Beijing 100191, China
[b] College of Aerospace Engineering, Chongqing University, Chongqing 400044, China
[c] School of Science, Harbin Institute of Technology, Shenzhen, Guangdong 518055, China

ARTICLE INFO

Keywords:
Linear viscoelasticity
Particle-reinforced composites
Constitutive modeling
Homogenization method
Numerical validation

ABSTRACT

In this paper, a novel micromechanics-based constitutive model is proposed for linear viscoelastic particle-reinforced composites based on a homogenization approach in the time domain. After decomposing the deformation into its volumetric and deviatoric parts, the long-term responses of the constituents are utilized to formulate the constitutive equations of the composites. The strain energy contributions of the constituents are computed from micromechanics principles to derive the effective constitutive model of the composites. Representative volume element models with various particle volume fractions are constructed to validate the constitutive model numerically. The effects of the particle volume fraction, strain rate, and elastic and viscous parameters on the effective viscoelastic behaviors of the composites and the creep performances are investigated. The results reveal that the proposed constitutive model can predict well the effective properties of linear viscoelastic particle-reinforced composites in the time domain. The experimental results are also employed to validate the proposed constitutive model in the frequency domain. The findings suggest that the constitutive model can also provide satisfactory predictions for the behaviors of the linear viscoelastic particle-reinforced composites in the frequency domain. After the constitutive model is validated, the composites, exhibiting full relaxation behaviors, are discussed.

1. Introduction

Viscoelastic particle-reinforced composites have been widely used in engineering practice owing to their excellent combination of high stiffness and damping properties (Dunn, 1995). As a fundamental problem, the prediction of the effective mechanical properties of viscoelastic particle-reinforced composites based on the mechanical properties of their constituents and the microstructures of the composites is still an active research area to date. The constitutive models of linear viscoelastic particle-reinforced composites in the literature can be generally classified into two categories, one based on Laplace transform and the other based on homogenization in the time domain.

The framework of Laplace transform was originally proposed by Hashin (1965) for linear viscoelastic heterogeneous materials, where the viscoelastic equations are transformed into the linear elastic regime using Laplace transforms. After carrying out a homogenization procedure in the Laplace domain, the equations are transformed inversely into the time domain to obtain the effective mechanical properties of the viscoelastic composites. Subsequently, various micromechanical models were employed to estimate the effective (fictional) elastic moduli of composites in the Laplace domain, such as those based on the self-consistent method (Laws and McLaughlin, 1978), the Mori-Tanaka method (Brinson and Lin, 1998) and the Hashin-Shtrikman bounds (DeBotton and Tevet-Deree, 2004). The complex moduli (Christensen, 1969; Hashin, 1970; Li and Weng, 1994) and damping properties (Azoti et al., 2013; Dunn, 1995) of different types of linear viscoelastic particle-reinforced composites were studied using different homogenization methods in the Laplace domain. Even though great advantages are offered by the Laplace transform to analyze the effective frequency-related properties of viscoelastic composites, the evaluation of their effective performances in the time domain is not straightforward. The main reason is that the (inverse) transform from the Laplace domain to the time domain is usually difficult to be accomplished since the effective elastic moduli in the Laplace domain are sometimes either not available in closed form or not simple enough to be analytically inverted. While, it is worth noting that, in some specific situations, such as the isotropic linear viscoelasticity considered in this paper, the analytical Laplace transform inversion is available for the particle-

* Corresponding authors.
E-mail addresses: z-guo@foxmail.com (Z. Guo), ltdong@buaa.edu.cn (L. Dong).

https://doi.org/10.1016/j.mechmat.2019.103228
Received 22 July 2019; Received in revised form 15 October 2019; Accepted 31 October 2019
Available online 01 November 2019

reinforced composites under the volumetric deformations, because the effective elastic bulk modulus is usually a simple closed-form rational function, for instance the composite-sphere model (Christensen, 1979). With regard to the deviatoric behaviors, while, the effective elastic shear modulus is usually not a simple closed-form function, so that the exact analytical Laplace transform inversion is difficult to be accomplished. However, the inverse transform is still can be implemented through employing some technical operations, such as model simplifications (Hashin, 1965), consideration of the specific viscoelastic model (Rougier et al., 1993), numerical inversion (Yi et al., 1998) and approximate inversion (Brenner et al., 2002).

To overcome the above limitation, some homogenization methods in the time domain have been proposed in the literature. Some of them characterize the interactions between the inclusions and the homogeneous medium for viscoelastic particle-reinforced composites, e.g., the additive-interaction law (Molinari et al., 1997), the translated-fields method (Paquin et al., 1999) and the exact-interaction law (Berbenni et al., 2015). Other approaches, such as variational incremental methods (Lahellec and Suquet, 2007a, b; Tressou et al., 2018), those combining the Laplace transform and internal variables (Ricaud and Masson, 2009), and full-field solutions (Seck et al., 2018), have been developed to characterize the effective behavior of linear viscoelastic particle-reinforced composites. In contrast to the models based on Laplace transform, homogenization methods in the time domain can offer an explicit description of the effective time-dependent response of viscoelastic composites. However, in homogenization methods, it is often very difficult to obtain closed-form constitutive equations of viscoelastic composites because of the introduction of time-dependent internal variables.

In this paper, a new homogenization method in the time domain is proposed to derive the constitutive model of linear viscoelastic particle-reinforced composites with explicit closed-form constitutive equations. The deformation is first decomposed into its volumetric and deviatoric parts. The long-term responses of the constituents are then utilized to formulate the constitutive equations of the composites. The strain energy contributions of the constituents are computed from micromechanics principles to derive the effective constitutive model of the composites. Unlike the homogenization methods in the time domain discussed above, the time-dependent internal variables are not introduced in the proposed method, which leads to a simple closed-form constitutive model of linear viscoelastic particle-reinforced composites. The resulting composite constitutive equation has the same form as that of composite's individual constituents. The simple closed form of the constitutive model provides an explicit description of the effective mechanical responses of composites in both the time and frequency domains. Representative volume element (RVE) models of viscoelastic particle-reinforced composites are also created to numerically validate the proposed constitutive model. Furthermore, the experimental results of the amorphous poly(ethylene)terephthalate (PET) reinforced with spherical glass beads (Cruz et al., 2009) are compared with the predictions of the proposed constitutive model.

This paper is organized as follows. In Section 2, the homogenization method in the time domain is proposed to derive the constitutive model of linear viscoelastic particle-reinforced composites. Section 3 presents comprehensive numerical validations of the proposed model. The experimental results in the literature are employed to validate the proposed constitutive model in Section 4. A detailed discussion of the full relaxation behaviors for the particle-reinforced composites is carried out in Section 5, and some concluding remarks are given in Section 6.

2. Constitutive formulation

2.1. Individual constituent

The particle-reinforced composites studied in this work are comprised of two linear viscoelastic constituents, whose constitutive behavior is generally described as

$$\sigma = \int_{-\infty}^{t} \mathrm{C}(t-\tau)\frac{d\varepsilon(\tau)}{d\tau}d\tau, \tag{1}$$

where $\boldsymbol{\sigma}$ and $\boldsymbol{\varepsilon}$ are the stress and strain tensors, respectively, and C represents the (fourth-order) stiffness tenor. The strain tensor $\boldsymbol{\varepsilon}$ can be additively decomposed into a volumetric part described by its trace, $\varepsilon_m = tr(\boldsymbol{\varepsilon})$, and a deviatoric part $\mathbf{e}$, defined so that, $\boldsymbol{\varepsilon} = (\varepsilon_m/3)\mathbf{I} + \mathbf{e}$, where $\mathbf{I}$ is the second-order identity tensor. Therefore, the mechanical behaviors of the materials can be characterized by superposing the volumetric and deviatoric performances. For isotropic materials, the constitutive Eq. (1) can be alternatively written as

$$\boldsymbol{\sigma} = \int_0^t k(t-\tau)\frac{d\varepsilon_m(\tau)}{d\tau}\,d\tau\,\mathbf{I} + 2\int_0^t \mu(t-\tau)\frac{d\mathbf{e}(\tau)}{d\tau}\,d\tau, \tag{2}$$

where $k(t)$ and $\mu(t)$ are defined as the relaxation bulk and shear moduli, respectively. Here, we also assume that both constituents are stress and strain-free when $t \le 0$. These relaxation moduli functions can be normalized as

$$k(t) = g_k(t)k^e, \quad \mu(t) = g_\mu(t)\mu^e, \tag{3}$$

where the material parameters, $k^e = \lim_{t\to\infty} k(t)$ and $\mu^e = \lim_{t\to\infty}\mu(t)$, refer to the corresponding long-term moduli, which relate to the purely elastic process when viscoelastic materials experience at sufficiently long (i.e., quasi-static) loading times. The dimensionless time-dependent relaxation functions $g_k(t)$ and $g_\mu(t)$, for the volumetric and deviatoric deformations, respectively, satisfy the condition that $\lim_{t\to\infty} g_k(t) = \lim_{t\to\infty} g_\mu(t) = 1$. Therefore, based on (3), the stress can be expressed as

$$\begin{aligned}\boldsymbol{\sigma} &= \int_0^t g_k(t-\tau)\frac{d\sigma_m^e(\tau)}{d\tau}\,d\tau\,\mathbf{I} + \int_0^t g_\mu(t-\tau)\frac{d\mathbf{s}^e(\tau)}{d\tau}\,d\tau \\ &= \int_0^t g_k(t-\tau)\frac{\partial^2 W_v^e[\boldsymbol{\varepsilon}(\tau)]}{\partial\boldsymbol{\varepsilon}\partial\tau}\,d\tau + \int_0^t g_\mu(t-\tau)\frac{\partial^2 W_d^e[\boldsymbol{\varepsilon}(\tau)]}{\partial\boldsymbol{\varepsilon}\partial\tau}\,d\tau.\end{aligned} \tag{4}$$

Here, $\sigma_m^e = k^e\varepsilon_m$ and $\mathbf{s}^e = 2\mu^e\mathbf{e}$ denote the referred elastic volumetric and deviatoric stresses, respectively, which correspond to the long-term moduli, k^e and μ^e. In addition, W_v^e and W_d^e are the referred elastic strain energy density functions (SEDFs) for the volumetric and deviatoric deformations of a given strain, respectively.

2.2. Homogenization approach

We consider an RVE of a heterogeneous material, which is macroscopically isotropic and occupies a volume V. Based on the homogenization framework developed by Hill (1972), the volumetric averages of the stress, strain and strain energy are computed as

$$\bar{\sigma} = \frac{1}{V}\int_V \boldsymbol{\sigma}\,dV, \quad \bar{\varepsilon} = \frac{1}{V}\int_V \boldsymbol{\varepsilon}\,dV, \quad \bar{W} = \frac{1}{V}\int_V W\,dV. \tag{5}$$

Substituting (4) into (5), the average stress of the linear viscoelastic particle-reinforced composites can be obtained as

$$\begin{aligned}\bar{\sigma} = \frac{1}{V}\Bigg\{&\int_0^t \left[g_k^m(t-\tau)\frac{\partial\left(\int_{V_m}\partial W_{mv}^e/\partial\boldsymbol{\varepsilon}\,dV\right)}{\partial\tau} + g_k^p(t-\tau)\frac{\partial\left(\int_{V_p}\partial W_{pv}^e/\partial\boldsymbol{\varepsilon}\,dV\right)}{\partial\tau}\right]d\tau \\ &+ \int_0^t \left[g_\mu^m(t-\tau)\frac{\partial\left(\int_{V_m}\partial W_{md}^e/\partial\boldsymbol{\varepsilon}\,dV\right)}{\partial\tau} + g_\mu^p(t-\tau)\frac{\partial\left(\int_{V_p}\partial W_{pd}^e/\partial\boldsymbol{\varepsilon}\,dV\right)}{\partial\tau}\right]d\tau\Bigg\},\end{aligned} \tag{6}$$

where V_m and V_p are the volumes of the matrix and particles, respectively. The scripts, m and p, in the material property functions, $g_k^m(t)$, $g_\mu^m(t)$, $g_k^p(t)$, $g_\mu^p(t)$, W_{mv}^e, W_{pv}^e, W_{md}^e, and W_{pd}^e represent the corresponding functions for the matrix and particles, respectively. According to Hill's homogenization theorem Hill, 1972), $\bar{W}(\bar{\varepsilon}) = \overline{W(\boldsymbol{\varepsilon})}$ can be treated as the effective SEDF of the composite since it describes the effective

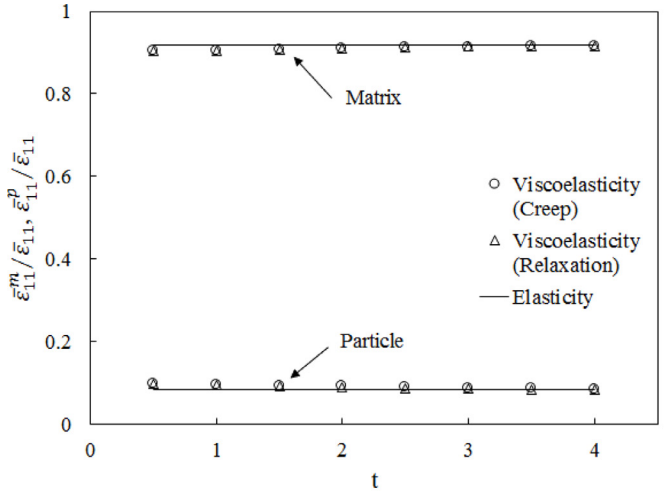

(a)

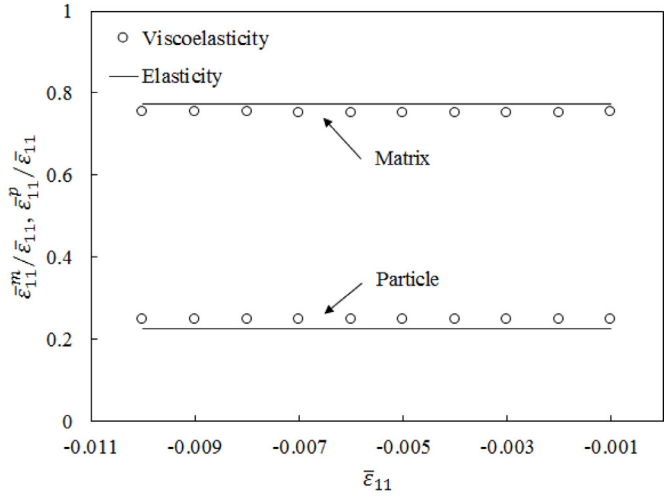

(b)

Fig. 1. A comparison between the effective viscoelastic strains (symbols) and the referred elastic strains (lines) of the matrix and particle for the particle-reinforced composites with $c = 0.3$ for (a) relaxation and creep under uniaxial tension ($E_p/E_m = 10$) and (b) proportionally applied uniaxial compression ($E_p/E_m = 2$).

mechanical behaviors of the "overall" composite. Hence, the volumetric average variables, $\bar{\sigma}$, $\bar{\varepsilon}$ and $\bar{W}$, are considered as the corresponding effective variables of the overall composite. Considering only the referred elastic parts of (6), the referred elastic stress can be represented as

$$\bar{\sigma}^e(t) = \frac{1}{V}\int_V \frac{\partial W^e[\boldsymbol{\varepsilon}(t)]}{\partial \boldsymbol{\varepsilon}(t)}\, dV = \frac{\partial \bar{W}^e[\bar{\varepsilon}(t)]}{\partial \bar{\varepsilon}(t)}, \tag{7}$$

where $\bar{W}^e[\bar{\varepsilon}(t)]$ is the effective SEDF of each constituent of the overall composite, respecting to the effective viscoelastic strain $\bar{\varepsilon}(t)$ of the corresponding constituent. Usually, the $\bar{\varepsilon}(t)$ is quite challengeable to be analytically computed for the viscoelastic particle-reinforced composites. Here, we consider a *referred elastic composite* of the same microstructure with the same load applied. The elastic moduli of the constituents of the referred elastic composite are the same as the long-term elastic moduli (i.e., $k^e = \lim_{t\to\infty} k(t)$ and $\mu^e = \lim_{t\to\infty} \mu(t)$) of the corresponding viscoelastic constituents of the original composite we studied. To simplify the theoretical difficulties, the effective strain $\bar{\varepsilon}^e$ of the referred elastic composite is employed to approximate the $\bar{\varepsilon}(t)$, that is,

Table 1
Normalized matrix and particle material parameters.

	E	ν	β_1	τ_1
Matrix	1	0.35	0.5	1
Particle	10	0.25	0.2	0.5

$\bar{W}^e[\bar{\varepsilon}(t)] \approx \bar{W}^e(\bar{\varepsilon}^e)$ is postulated. We note that the $\bar{\varepsilon}^e$ can be regarded as the effective long-term strain, $\lim_{t\to\infty}[\bar{\varepsilon}(t)] = \bar{\varepsilon}^e$, under a given load. Fig. 1a compares the effective elastic and viscoelastic strains, computed from the FEM simulations, for the matrix and particle phases of the composite with $c = 0.3$ under the relaxation and creep. Uniaxial tensions are proportionally applied to $\bar{\varepsilon}_{11}$ (or $\bar{\sigma}_{11}$) $= 0.01$ up to the normalized time $t = 1$ and then held constant until $t = 4$. The normalized material parameters are presented in Table 1. This figure shows that the $\bar{\varepsilon}$ computed from the relaxation and creep are almost superposed. They are very close to the $\bar{\varepsilon}^e$, which obviously keeps constant, during the entire loading process. This implies a good agreement between $\bar{\varepsilon}$ and $\bar{\varepsilon}^e$. Fig. 1b presents the comparison of $\bar{\varepsilon}$ and $\bar{\varepsilon}^e$ for the matrix and particle phases of the composites with comparable constituent's stiffness (i.e., $E_p/E_m = 2$) undergoing uniaxial compression (the strain rate $\dot{\varepsilon}_{11} = 0.01/s$). For the case of comparable constituent's stiffness, the differences between the $\bar{\varepsilon}$ and $\bar{\varepsilon}^e$ are slightly larger due to the stronger strain interaction between the matrix and particles, while the values are well below 3.5%. Therefore, it is reliable to use $\bar{\varepsilon}^e$ to approximate $\bar{\varepsilon}$ for both the constituents of the linear viscoelastic particle-reinforced composites.

Based on (7) and the elastic approximation, the constitutive equation given by (6) can be reformulated as

$$\begin{aligned}\bar{\sigma} = &\int_0^t \left\{ g_k^m(t-\tau)\frac{\partial^2 \bar{W}^e_{mv}[\bar{\varepsilon}^e(\tau)]}{\partial \bar{\varepsilon}^e \partial \tau} + g_k^p(t-\tau)\frac{\partial^2 \bar{W}^e_{pv}[\bar{\varepsilon}^e(\tau)]}{\partial \bar{\varepsilon}^e \partial \tau} \right\} d\tau \\ &+ \int_0^t \left\{ g_\mu^m(t-\tau)\frac{\partial^2 W^e_{md}[\bar{\varepsilon}^e(\tau)]}{\partial \bar{\varepsilon}^e \partial \tau} + g_\mu^p(t-\tau)\frac{\partial^2 \bar{W}^e_{pd}[\bar{\varepsilon}^e(\tau)]}{\partial \bar{\varepsilon}^e \partial \tau} \right\} d\tau,\end{aligned} \tag{8}$$

where $\bar{W}^e_{mv}(\bar{\varepsilon}^e) = [\int_{V_m} W^e_{mv}(\boldsymbol{\varepsilon}^e)\, dV]/V$, $\bar{W}^e_{pv}(\bar{\varepsilon}^e) = [\int_{V_p} W^e_{pv}(\boldsymbol{\varepsilon}^e)\, dV]/V$, $\bar{W}^e_{md}(\bar{\varepsilon}^e) = [\int_{V_m} W^e_{md}(\boldsymbol{\varepsilon}^e)\, dV]/V$, and $\bar{W}^e_{pd}(\bar{\varepsilon}^e) = [\int_{V_p} W^e_{pd}(\boldsymbol{\varepsilon}^e)\, dV]/V$ represent the effective SEDFs of the matrix and particles of the referred elastic composites for the volumetric and deviatoric deformations, respectively.

Here, we define $R_v = \bar{W}^e_{pv}/\bar{W}^e_v$ and $R_d = \bar{W}^e_{pd}/\bar{W}^e_d$ as the effective strain energy ratios of the particle to that of the composite for the volumetric and deviatoric deformations, respectively, where $\bar{W}^e_v(\bar{\varepsilon}^e) = [\int_V W^e_v(\boldsymbol{\varepsilon}^e) dV]/V = \bar{W}^e_{pv}(\bar{\varepsilon}^e) + \bar{W}^e_{mv}(\bar{\varepsilon}^e)$ and $\bar{W}^e_d(\bar{\varepsilon}^e) = [\int_V W^e_d(\boldsymbol{\varepsilon}^e)\, dV]/V = \bar{W}^e_{pd}(\bar{\varepsilon}^e) + \bar{W}^e_{md}(\bar{\varepsilon}^e)$ denote the effective SEDFs of the composite under volumetric and deviatoric deformations, respectively. For the volumetric deformation, R_v is independent of the elastic volumetric strain $\varepsilon^e_m = tr(\boldsymbol{\varepsilon}^e)$ due to the linearity of the composite system. For the deviatoric deformation, it can also be proven that R_d is independent of the elastic deviatoric strain tensor $\mathbf{e}^e = \boldsymbol{\varepsilon}^e - (\varepsilon^e_m/3)\mathbf{I}$ using the isotropy assumption of the composites. That is, for a given composite, R_v and R_d are constants. Therefore, employing R_v and R_d, the effective stress tensor of the composite given by (8) can be reformulated as

$$\begin{aligned}\bar{\sigma} = &\int_0^t [R_v g_k^p(t-\tau) + (1-R_v) g_k^m(t-\tau)] \frac{\partial^2 \bar{W}^e_v}{\partial \bar{\varepsilon}^e \partial \tau}\, d\tau \\ &+ \int_0^t \left[R_d g_\mu^p(t-\tau) + (1-R_d) g_\mu^m(t-\tau) \right] \frac{\partial^2 \bar{W}^e_d}{\partial \bar{\varepsilon}^e \partial \tau}\, d\tau.\end{aligned} \tag{9}$$

Eq. (9) can be written in a similar format to (2) for an individual constituent. Thus,

$$\bar{\sigma} = \int_0^t \bar{g}_k(t-\tau)\bar{k}^e \frac{\partial \bar{\varepsilon}_m}{\partial \tau}\, d\tau\, \mathbf{I} + 2\int_0^t \bar{g}_\mu(t-\tau)\bar{\mu}^e \frac{\partial \bar{\mathbf{e}}}{\partial \tau}\, d\tau. \tag{10}$$

Here, $\bar{k}^e$ and $\bar{\mu}^e$ represent the effective elastic bulk and shear moduli,

respectively, while $\bar{\varepsilon}_m = tr(\bar{\varepsilon})$ and $\bar{\mathbf{e}} = \bar{\varepsilon} - (\bar{\varepsilon}_m/3)\mathbf{I}$ denote the volumetric and deviatoric effective strains of a given effective strain tensor $\bar{\varepsilon}$, respectively. The effective dimensionless relaxation functions of the composite are defined as

$$\bar{g}_k(t) = R_v g_k^p(t) + (1 - R_v) g_k^m(t),$$
$$\bar{g}_\mu(t) = R_d g_\mu^p(t) + (1 - R_d) g_\mu^m(t). \tag{11}$$

We note that it is the analogy between the constitutive model of the composite and those of the individual constituents that greatly facilitates the study of the effective mechanical behavior of viscoelastic particle-reinforced composites in both the time and frequency domains.

In this paper, the generalized Maxwell model is used to describe the linear viscoelastic responses of the matrix and particles. The dimensionless relaxation function for the generalized Maxwell model is given as a Prony series (Lakes, 2009)

$$g(t) = 1 + \sum_{\alpha=1}^{n} \beta_\alpha e^{-t/\tau_\alpha}, \tag{12}$$

where β_α is the dimensionless viscous parameter, and τ_α refers to the relaxation time. The integer, n, represents the number of terms in the series. Therefore, based on (11), the effective dimensionless relaxation functions for the volumetric and deviatoric deformations can be derived when their effective strain energy ratios of the particles to composite, R_v and R_d, are determined. After the effective elastic bulk and shear moduli of the composite are obtained, the effective stress $\bar{\sigma}$ of the linear viscoelastic particle-reinforced composite can then be computed according to (10).

It is worth noting that no microstructure limitation for the particle-reinforced composites is introduced in constructing the homogenization method to derive the constitutive model of the linear viscoelastic particle-reinforced composites. It implies that the proposed method can be applied to the composites reinforced by any particle shape and distribution. However, it is quite challengeable to determine the effective strain energy ratios, R_v and R_d, and the effective moduli, $\bar{k}^e$ and $\bar{\mu}^e$, for the composites reinforced with non-spherical or non-randomly distributed particles. Therefore, this paper limits on the discussions for the linear viscoelastic composites with spherical and randomly distributed particles.

2.3. Determinations of R_v, R_d, $\bar{k}^e$ and $\bar{\mu}^e$

We first compute the effective elastic bulk modulus $\bar{k}^e$ and the effective volumetric strain energy ratio of the particle to composite R_v. Using the classical composite-sphere model, the effective elastic bulk modulus can be expressed as (Christensen, 1979)

$$\bar{k}^e = k_m^e + \frac{c(k_p^e - k_m^e)}{1 + (1-c)\left[(k_p^e - k_m^e)/\left(k_m^e + \frac{4}{3}\mu_m^e\right)\right]}, \tag{13}$$

where k_p^e, k_m^e and μ_m^e are the elastic bulk modulus of the particle, the matrix and the elastic shear modulus of the matrix, respectively. Furthermore, the parameter c is the volume fraction of the particles. The effective strain energy of the particle and matrix for the composite sphere subjected to a hydrostatic pressure p can be computed as (Christensen, 1979)

$$\bar{W}_p^e = \frac{9}{2} c k_p^e A_p^2 p^2,$$
$$\bar{W}_m^e = \frac{3}{2}\left[3k_m^e A_m^2 (1-c) - 4\mu_m^e B_m^2 \left(1 - \frac{1}{c}\right)\right] p^2. \tag{14}$$

The parameters in (14) are determined as

$$A_p = \frac{L}{\mu_m^e} - \frac{1}{4c\mu_m^e} + \frac{3k_m^e L}{16c(\mu_m^e)^2}, \quad A_m = \frac{L}{4\mu_m^e}, \quad B_m = \frac{3k_m^e}{4\mu_m^e} A_m - \frac{A_m}{L},$$
$$L = \frac{3k_p^e + 4\mu_m^e}{3c(k_p^e - k_m^e) + \frac{9}{4}\frac{k_p^e k_m^e}{\mu_m^e} + 3k_m^e}. \tag{15}$$

The effective volumetric strain energy ratio of the particles to composite R_v is calculated as

$$R_v = \frac{\bar{W}_p^e}{\bar{W}_p^e + \bar{W}_m^e} = \frac{9ck_p^e A_p^2}{9ck_p^e A_p^2 + 3\left[3k_m^e(1-c)A_m^2 - 4\mu_m^e\left(1 - \frac{1}{c}\right)B_m^2\right]}. \tag{16}$$

It has been numerically verified by Segurado and Llorca (2002) that the three-phase model (TPM) (Christensen and Lo, 1979) can provide accurate estimates for the effective shear moduli of linear elastic particle-reinforced composites. Consequently, the TPM is utilized to approximate the effective elastic shear modulus $\bar{\mu}^e$, as well as the effective deviatoric strain energy ratio of the particles to composite R_d. The TPM offers a complicated but closed-form formulation of $\bar{\mu}^e$, which can be easily computed numerically. Based on the TPM, the strain fields in the particles and the matrix under simple shear can be also determined. The expression of $\bar{\mu}^e$ and the formulation of the strain fields are not given explicitly here, since the detailed expressions can be found in (Christensen and Lo, 1979). After the strain fields are determined, the effective SEDFs of the particles $\bar{W}_p^e$ and matrix $\bar{W}_m^e$, can be obtained as

$$\bar{W}_p^e = \frac{1}{2V}\int_{V_p} (C_p : \boldsymbol{\varepsilon}) : \boldsymbol{\varepsilon}\, dV, \quad \bar{W}_p^e = \frac{1}{2V}\int_{V_m} (C_m : \boldsymbol{\varepsilon}) : \boldsymbol{\varepsilon}\, dV, \tag{17}$$

where C_p and C_m are the stiffness tensors of the particles and matrix, respectively. The deviatoric strain energy ratio of the particles to the composite's is then obtained as

$$R_d = \frac{\bar{W}_p^e}{\bar{W}_p^e + \bar{W}_m^e}. \tag{18}$$

Thus, the value R_d can now be computed in terms of the particle volume fraction c, for composites with various particle/matrix stiffness contrasts (see Fig. 2). After R_v, R_d, $\bar{k}^e$ and $\bar{\mu}^e$ are obtained, the effective stress $\bar{\sigma}$ of linear viscoelastic particle-reinforced composites can be computed using the constitutive Eq. (10).

3. Numerical validation

3.1. RVE models and finite element simulations

The RVE models adopted in Guo et al. (2014) are employed in this paper to numerically validate the proposed constitutive model. Each cuboidal RVE model contains 27 randomly distributed non-overlapping

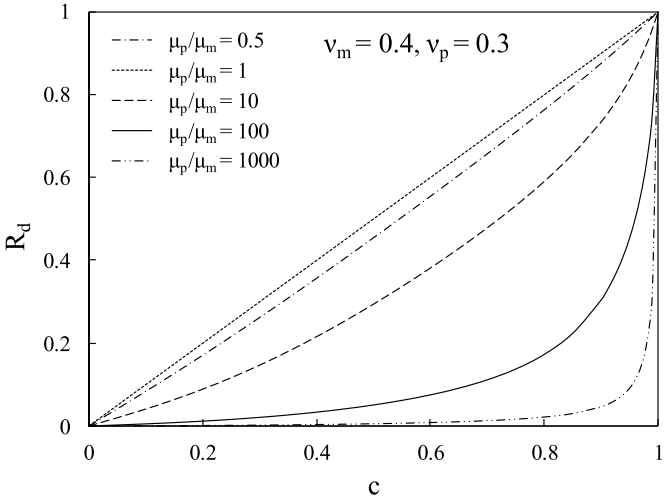

Fig. 2. Effective strain energy ratio between the particles and the composite, R_d, for the particle-reinforced composites undergoing isochoric deformations as a function of the particle volume fraction c, for different particle/matrix stiffness ratios μ_p/μ_m.

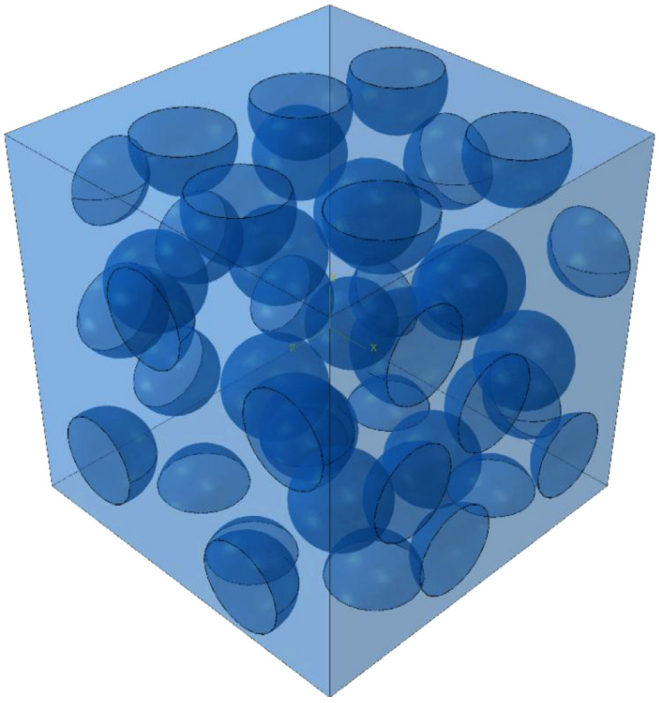

Fig. 3. A sample of the RVE models ($c = 0.2$) with periodic microstructures for the viscoelastic particle-reinforced composites.

same-sized spheres (Fig. 3). Here, nine RVE models with three different particle volume fractions (i.e., $c = 0.1$, 0.2 and 0.3, and 3 models for each value of c) are modelled using finite element (FE) techniques. The periodic microstructures of the RVE models are enforced and the periodic boundary conditions (PBCs) are applied in every RVE model. All the FE simulations are performed using the commercial code ABAQUS/Standard with the geometric nonlinearity switched on. About 80,000 quadratic tetrahedral elements (element type C3D10 in ABAQUS) and approximately 120,000 nodes are used to model each RVE. The isotropy of the RVE models as well as the level of mesh refinement have been comprehensively verified by Guo et al. (2014). For more details of the RVE models, PBCs, meshes and evaluation of the macroscopic constitutive behaviors, see Guo et al. (2014).

3.2. Effect of particle content

Stress relaxation loading conditions under uniaxial tension and simple shear are applied to all the RVE models to validate the constitutive model. Without loss of generality, the normalized material parameters are utilized, and the normalizing factors are set as the corresponding matrix material parameters. The tensile and shear strains are proportionally applied up to $\varepsilon_{11} = \varepsilon_{22} = 0.01$ within a normalized time of $t = 1$. After that, strains are held constant until $t = 4$. The normalized material parameters of the particles and the matrix (i.e., Young's modulus (E), Poisson's ratio (ν), viscous parameter (β_1) and relaxation time (τ_1)) are defined in Table 1. We note that, in the numerical simulations, the dimensionless viscous parameters and relaxation time defined in (12), namely β_α and τ_α, respectively, for the volumetric and deviatoric deformations are assumed to be the same, which implies that the constituents exhibit the same viscous behavior whether they undergo volumetric or deviatoric deformations. The stresses σ_{11} and σ_{12} for the stress relaxation under uniaxial tension and simple shear are plotted in Fig. 4 against the loading time t. For each value of c, the results obtained from the three corresponding RVE models show a good correlation, with less than 2.8% and 1.3% discrepancies for the relaxations under uniaxial tensions and simple shears, respectively. This suggests that the RVE models are large enough for the effective

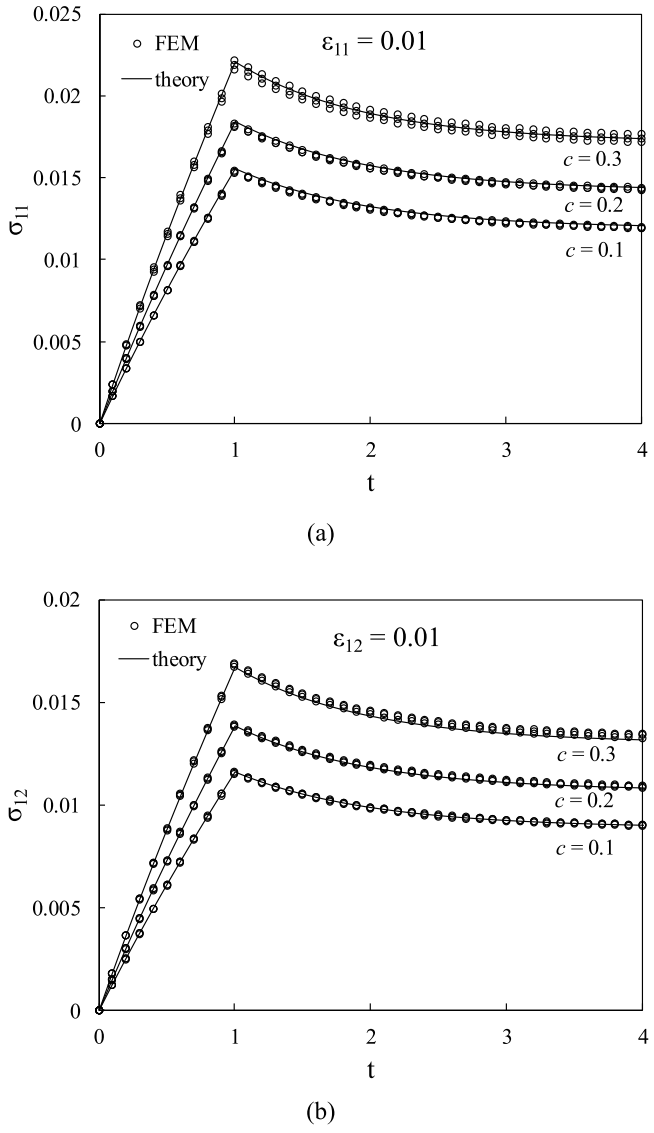

Fig. 4. A comparison between the stresses computed with the constitutive model (lines) and the FEM simulations (symbols) for different particle volume fractions for (a) uniaxial tension, and (b) simple shear as a function of loading time.

response of the composites to be predicted accurately. The predictions of the proposed constitutive model are plotted in Fig. 4 for comparison. Here, it can be seen that the theoretical predictions coincide very well with all the FEM results, with the maximum discrepancy being 1.3%. These results reveal that the constitutive model can correctly capture the relaxation behavior of the viscoelastic particle-reinforced composite with particle volume fractions ranging from 10% to 30%.

3.3. Effect of strain rate

We apply uniaxial tensile deformations to the RVE models with $c = 0.3$ and four different strain rates (i.e., $\dot{\varepsilon}_{11} \to 0$, $\dot{\varepsilon}_{11} = 0.001$, 0.01 and 0.1/s) to further validate the constitutive model. Here, $\dot{\varepsilon}_{11} \to 0$ indicates a sufficiently long process related to a purely elastic response. Again, the material constants defined in Table 1 are used. The FEM results of the stress σ_{11} vs. the strain ε_{11} for different strain rates are presented in Fig. 5. It can be seen that the results obtained from the three RVE models agree well with each other for the different strain rates, with the maximum relative differences being less than 1.3%, and that the stresses increase with strain rate, as expected. We note that the

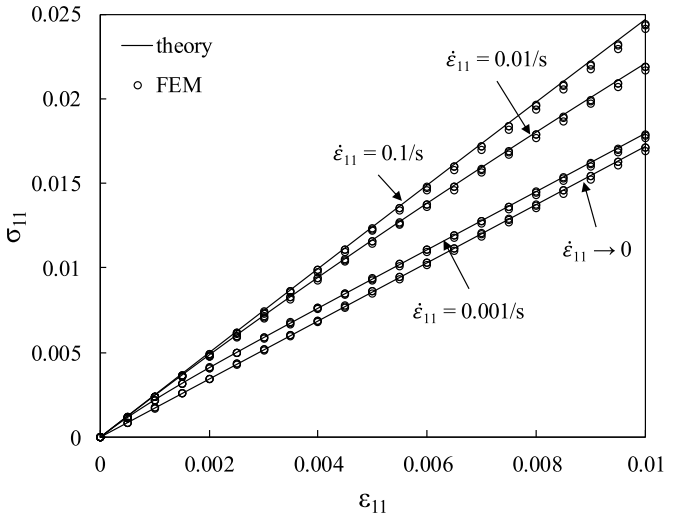

Fig. 5. A comparison between the nominal stresses predicted by the constitutive model under uniaxial tension with $c = 0.3$ (lines) and the FEM results (symbols) for different strain rates.

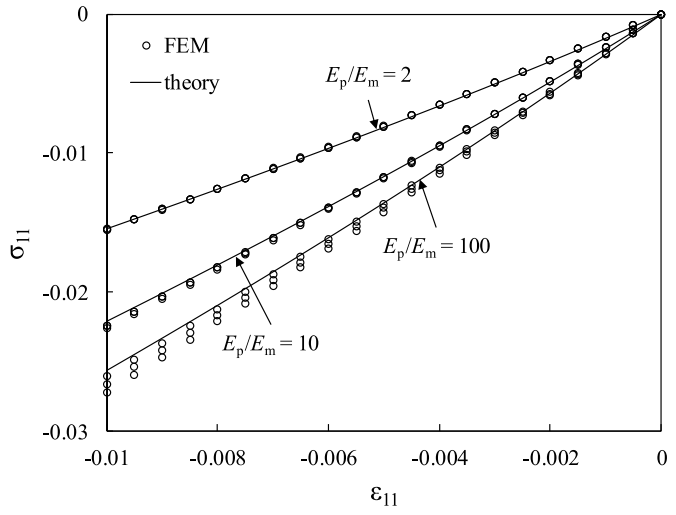

Fig. 6. The nominal stresses computed from the RVE models with $c = 0.3$ (symbols) under uniaxial compression are compared with the constitutive model predictions (lines) for different particle/matrix stiffness ratios.

nonlinearity of the effective tensile behaviors under different strain rates is seen to be weak. This phenomenon mainly results from the small deformation applied as well as the low viscous parameter and relaxation time defined. A comparison between the stresses predicted by the constitutive model and the FEM results is shown in Fig. 5. The results show that the theoretical and numerical results are almost superposed at the relatively small strain rate of $\dot{\varepsilon}_{11} \leq 0.001$/s. As the strain rate increases, the constitutive model slightly overestimates the stress predicted by the FEM, with the relative differences well below 1.6%. These results demonstrate the capability of the constitutive model to predict accurately the strain rate sensitivity of the composite behavior.

3.4. Effect of elastic parameters

In this subsection, we explore the effect of the elastic parameters (i.e., Young's modulus and Poisson's ratio) of both the matrix and the particles on the effective composite behavior. Here, the ratios $E_p/E_m = 2$, 10 and 100 and $c = 0.3$ are employed in the RVE simulations to study the effect of the particle/matrix stiffness contrast. The other material parameters are set to be the same as those listed in Table 1. A uniaxial compression loading condition with a strain rate of $\dot{\varepsilon}_{11} = 0.01$/s is considered in the FEM simulations. The corresponding stress-strain curves for different stiffness ratios are plotted in Fig. 6. The numerical RVE results demonstrate that a somehow larger divergence at the high particle/matrix stiffness contrast of $E_p/E_m = 100$, viz. less than 4.2%, when compared with the lower stiffness ratio results. The stresses predicted by the constitutive model agree well with the FEM results, with the maximum relative differences being well below 1.8% when $E_p/E_m \leq 10$, and 3.8% when $E_p/E_m = 100$.

After investigating the stiffness contrast effect, the effect of the matrix and particle Poisson's ratios on the effective composite response was explored. Here, values of $\nu_p = 0.25$ for the particle, and $\nu_m = 0.35$, 0.45 and 0.495 for the matrix are used. The other material constants are the same as those listed in Table 1. The plane-strain uniaxial tension (i.e., uniaxial tension in ε_{11}, constraint in ε_{33} and free in ε_{22}) with a strain rate of $\dot{\varepsilon}_{11} = 0.01$/s was applied to the RVE models with $c = 0.3$. The stresses in both the tensile, σ_{11}, and the constrained, σ_{33}, directions are plotted in Fig. 7 as the functions of the tensile strain ε_{11}. Again, the numerical results from the three RVE models demonstrate a good agreement for σ_{11} and σ_{33}, exhibiting a maximum relative differences of 3.8% and 5.5%, respectively. These results also reveal a good correlation between the theoretical predictions and the numerical results when $\nu_m = 0.35$. When the matrix tends to be incompressible ($\nu_m \to 0.5$), the constitutive model slightly overestimates (< 2.7%) the stresses along both the tensile and constrained directions, which suggests that the constitutive can predict well the effective behaviors of the RVE models with a composite matrix having a range of Poisson's ratios.

3.5. Effect of the viscous parameters

To study the effect of the viscous parameters on the effective viscoelastic responses of the particle-reinforced composites, three sets of viscous parameters are used in the RVE models, as defined in Table 2. First, we consider the composite as purely elastic. Then we investigate the composite with purely elastic particles and a viscoelastic matrix using the second set of parameters. In the third set of parameters, both the particle and the matrix are modelled as viscoelastic materials. The Young's moduli and Poisson's ratios of the matrix and particles are listed in Table 1. Plane-strain compression with $\dot{\varepsilon}_{11} = 0.01$/s was applied to the three RVE models with $c = 0.3$. The computed compression stress σ_{11} and constraining stress σ_{33} from the three RVE models are consistent with the constitutive model predictions, exhibiting a maximum discrepancy of 4.3% (Fig. 8). The theoretical predictions agree well with the numerical results, and the maximum relative difference between the models' predictions and the numerical results is about 2.2%. Thus it can be concluded that the proposed model is capable of predicting well the effective behaviors of the composite assuming different combinations of elastic and viscoelastic properties for the particle and matrix.

3.6. Creep behaviors

The constitutive model of (10) for the linear viscoelastic particle-reinforced composites presents an integral function with respect to the variable of the effective strain, which provides the direct computation of the effective stress for a given strain history. For the case of applying stress, the numerical iteration can be carried out to find the solution of the strain response. Strain creep loadings under uniaxial tension are applied to the RVE models of $c = 0.3$ to further validate the constitutive model. The normalized tensile stress is proportionally applied up to $\sigma_{11} = 0.01$ and then held constant until $t = 4$. The material constants are defined as the values given in Table 1. The strains computed from the RVE models as well as the constitutive model are presented in Fig. 9, as the functions of the loading time. Again, the FEM results simulated from the three RVE models demonstrate the good agreement. The strain estimated by the constitutive model coincides well with the numerical results, showing the relative difference of less than 3.6%. It implies that

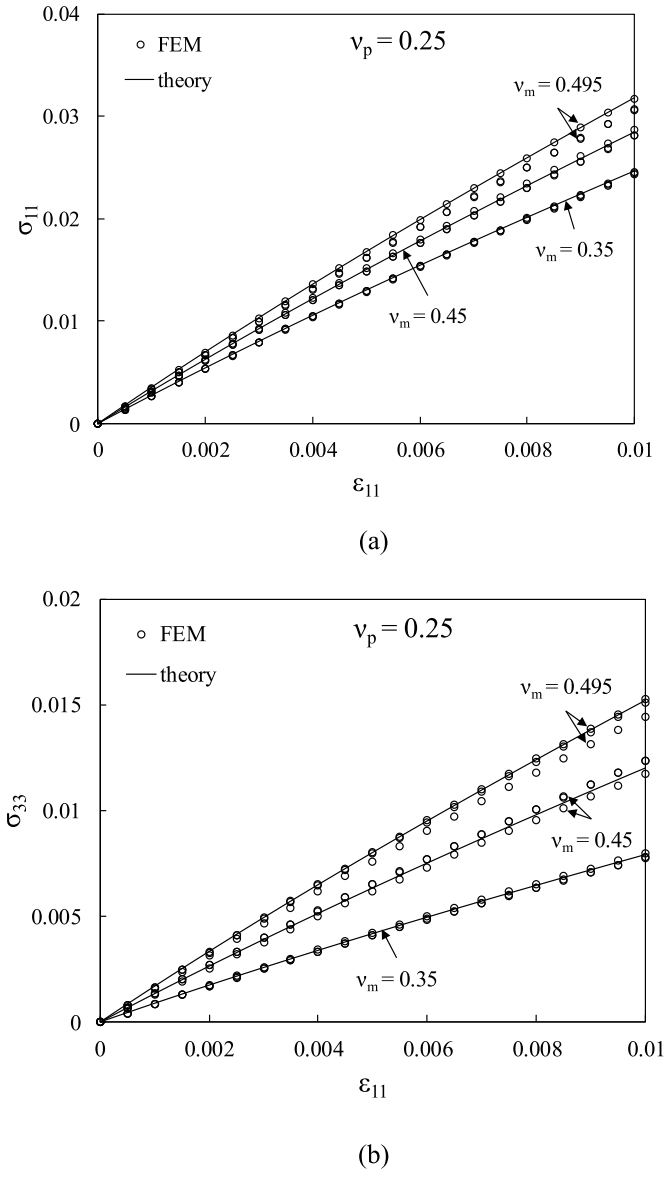

Fig. 7. Comparisons between the stresses along the (a) tensile direction σ_{11}, and the (b) constrained direction σ_{33}, computed from the constitutive (lines) and the RVE (symbols) models when subjected to plane-strain tension as a function of the tensile strain ε_{11}, and for different Poisson's ratios of the matrix.

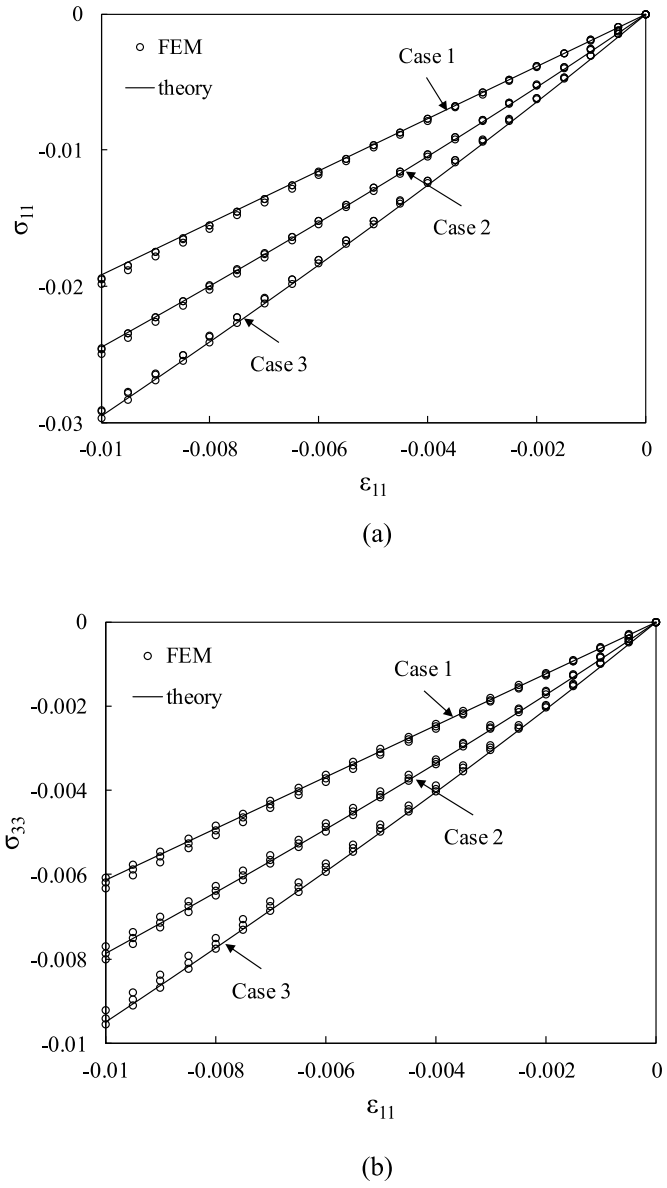

Fig. 8. Comparisons between the stresses along (a) the tensile direction σ_{11}, and (b) the constrained direction σ_{33}, computed from the RVE models (symbols) and the constitutive model predictions (lines) under plane-strain compression with $c = 0.3$ for the various combinations of elastic and viscoelastic parameters for the particle and matrix.

Table 2
Normalized matrix and particle viscous parameters*.

	β_{m1}	τ_{m1}	β_{m2}	τ_{m2}	β_{m3}	τ_{m3}	β_{p1}	τ_{p1}
Case 1	\	\	\	\	\	\	\	\
Case 2	0.5	1	\	\	\	\	\	\
Case 3	0.5	1	0.2	10	0.1	100	0.2	0.5

* The symbol "\" represents no value in this table.

the constitutive model can also offer sufficiently good predictions of the creep behaviors for the linear viscoelastic particle-reinforced composites.

4. Experimental validation

As the proposed model is numerically validated in the time domain, it is then utilized to predict the effective behaviors of the PET reinforced by spherical glass beads in the frequency domain. Under the steady-state harmonic oscillatory strains, the storage moduli (real parts) and loss moduli (imaginary parts) for the complex shear modulus $\mu^* = \mu' + i\mu''$ and bulk modulus $k^* = k' + ik''$ are computed by (Lakes, 2009)

$$\mu'(\omega) = \mu^e + \omega \int_0^\infty [\mu(\tau) - \mu^e]\sin(\omega\tau)\, d\tau, \tag{19}$$

$$\mu''(\omega) = \omega \int_0^\infty [\mu(\tau) - \mu^e]\cos(\omega\tau)\, d\tau, \tag{20}$$

$$k'(\omega) = k^e + \omega \int_0^\infty [k(\tau) - k^e]\sin(\omega\tau)\, d\tau, \tag{21}$$

$$k''(\omega) = \omega \int_0^\infty [k(\tau) - k^e]\cos(\omega\tau)\, d\tau, \tag{22}$$

where ω is the angular frequency of the applied strains. Owing to the analogy between the constitutive models of the composites and their individual constituents, the effective storage and loss moduli for the composites under deviatoric and volumetric deformations can be

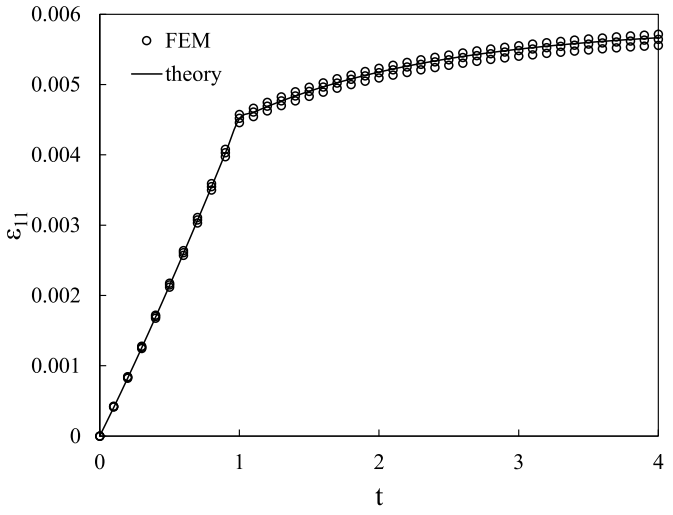

Fig. 9. A comparison between the strains computed with the constitutive model (lines) and the FEM simulations (symbols) for the models of $c = 0.3$ for the creep behaviors under uniaxial tension.

straightforwardly derived, with the explicit forms of

$$\bar{\mu}' = \bar{\mu}^e + \omega\bar{\mu}^e\left[(1-R_d)\sum_{\alpha_m=1}^{n_m}\beta_{\alpha_m}\frac{\omega\tau_{\alpha_m}^2}{1+\omega^2\tau_{\alpha_m}^2} + R_d\sum_{\alpha_p=1}^{n_p}\beta_{\alpha_p}\frac{\omega\tau_{\alpha_p}^2}{1+\omega^2\tau_{\alpha_p}^2}\right], \tag{23}$$

$$\bar{\mu}'' = \omega\bar{\mu}^e\left[(1-R_d)\sum_{\alpha_m=1}^{n_m}\beta_{\alpha_m}\frac{\tau_{\alpha_m}}{1+\omega^2\tau_{\alpha_m}^2} + R_d\sum_{\alpha_p=1}^{n_p}\beta_{\alpha_p}\frac{\tau_{\alpha_p}}{1+\omega^2\tau_{\alpha_p}^2}\right], \tag{24}$$

$$\bar{k}' = \bar{k}^e + \omega\bar{k}^e\left[(1-R_v)\sum_{\alpha_m=1}^{n_m}\beta_{\alpha_m}\frac{\omega\tau_{\alpha_m}^2}{1+\omega^2\tau_{\alpha_m}^2} + R_v\sum_{\alpha_p=1}^{n_p}\beta_{\alpha_p}\frac{\omega\tau_{\alpha_p}^2}{1+\omega^2\tau_{\alpha_p}^2}\right], \tag{25}$$

$$\bar{k}'' = \omega\bar{k}^e\left[(1-R_v)\sum_{\alpha_m=1}^{n_m}\beta_{\alpha_m}\frac{\tau_{\alpha_m}}{1+\omega^2\tau_{\alpha_m}^2} + R_v\sum_{\alpha_p=1}^{n_p}\beta_{\alpha_p}\frac{\tau_{\alpha_p}}{1+\omega^2\tau_{\alpha_p}^2}\right]. \tag{26}$$

The experimental results reported by Cruz et al. (2009) are employed. The mechanical responses of the PET matrix under shears with different frequencies ω can be fitted well using the linear viscoelastic model with the form of Prony series (12) (Fig. 10a), and the fitted material parameters are presented in Table 3. The reinforcements of glass beads are considered as linear elastic materials, whose Young's modulus and Poisson's ratio are $E_p = 28$GPa and $\nu_p = 0.2$ (Cruz et al., 2009), respectively. The experimental results as well as the theoretical predictions from the proposed model for the effective storage and loss shear moduli of the composites with $c = 0.15$ and 0.27 are presented in Fig. 10b and c, respectively, as the functions of the frequency ω. For comparison, the theoretical estimates from the Mori-Tanaka model (MT) (Benveniste, 1987) combining the Hashin's elastic-viscoelastic correspondence principle (Hashin, 1970) are also included in the figures. As can be seen, the two theoretical predictions demonstrate the same tendency with the experiments. For $c = 0.15$, the effective storage and loss shear moduli computed from the two theoretical model are nearly the same. However, both of them are seen to underestimate the experimental results. For $c = 0.27$, the effective storage and loss shear moduli estimated from the proposed model are fairly better than that predicted from the MT. It is fair to conclude that the effective storage and loss shear moduli are well predicted by the proposed model when the PET is reinforced with spherical elastic glass beads up to nearly 30%. As expected, the effect of the volume fraction of the beads are

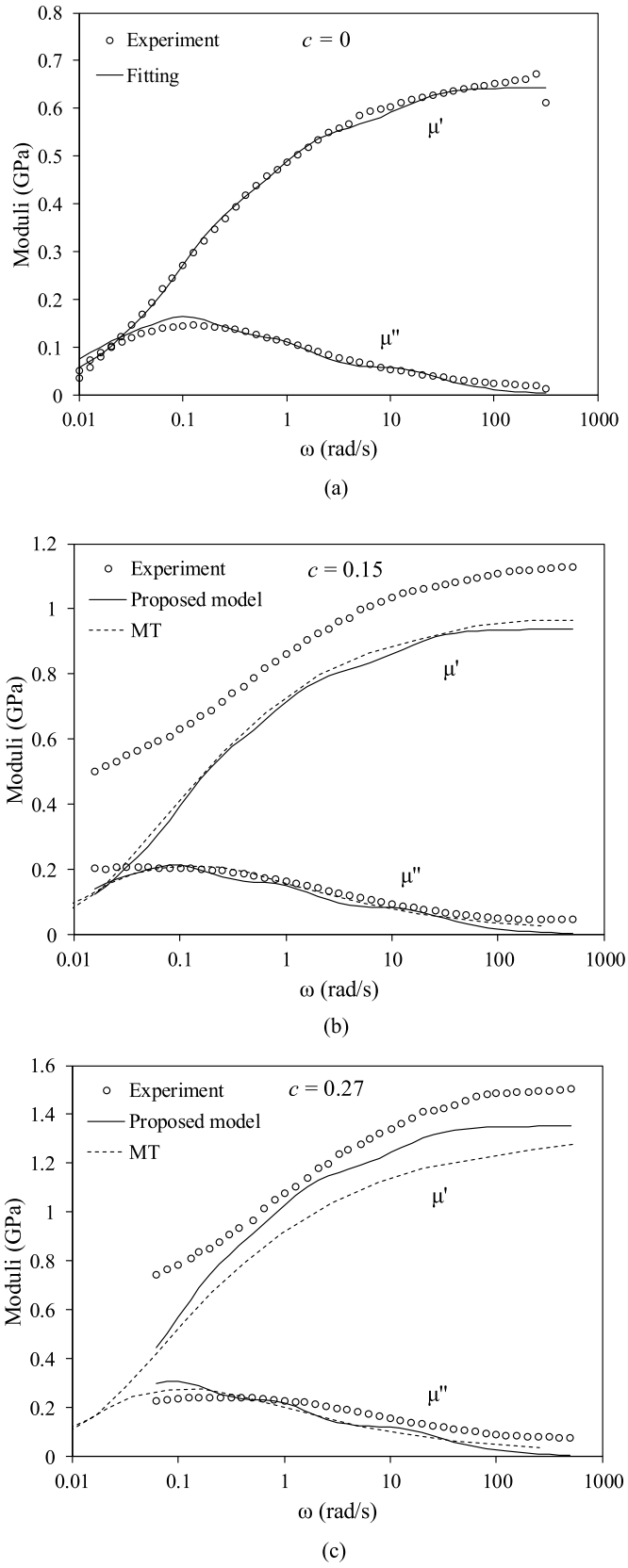

Fig. 10. Comparisons of effective storage and loss shear moduli from the experiments (symbols), proposed model (solid lines) and MT (dash lines) for (a) pure PET, (b) PET reinforced by 15 vol% glass beads, and (c) PET reinforced by 27 vol% glass beads.

Table 3
The material parameters of the PET.

μ_m (GPa)	ν_m	β_{m1}	τ_{m1} (s)	β_{m2}	τ_{m2} (s)
0.032	0.48	6.49	10.02	4.61	1.1
β_{m3}	τ_{m3} (s)	β_{m4}	τ_{m4} (s)	β_{m5}	τ_{m5} (s)
4.02	48.3	2.62	0.08	1.36	5.32

better assessed by the proposed model as compared to Mori-Tanaka.

5. Full relaxation behaviors

The proposed constitutive model considers that the effective behaviors of the viscoelastic composites can be decomposed into the corresponding time-dependent and long-term parts, which implies that the performances of the composites will bound to the (non-zero) long-term states as the loading time tends to be infinity. However, for some viscoelastic materials, their behaviors will be fully relaxed, so that the constitutive model fails to estimate the effective performances of the composites consisting of this kind of viscoelastic materials. To overcome this limitation, the instantaneous behaviors, instead of the long-term behaviors, are utilized to reformulate the constitutive model.

Employing the instantaneous (time-independent) bulk modulus $k^0 = \lim_{t\to 0} k(t)$ and shear modulus $\mu^0 = \lim_{t\to 0}\mu(t)$, the relaxation moduli functions can be alternatively normalized as

$$k(t) = g_k^0(t)k^0, \quad \mu(t) = g_\mu^0(t)\mu^0, \tag{27}$$

where g_k^0 and g_μ^0 satisfy the condition that $\lim_{t\to 0} g_k^0(t) = \lim_{t\to 0} g_\mu^0(t) = 1$ and relate to the time-dependent relaxation functions for the volumetric and deviatoric deformations, respectively. Therefore, based on the instantaneous moduli, the constitutive model of the individual constituents can be rewritten as

$$\boldsymbol{\sigma} = \int_0^t g_k^0(t-\tau)k^0\frac{d\varepsilon_m(\tau)}{d\tau}\,d\tau\,\mathbf{I} + 2\int_0^t g_\mu^0(t-\tau)\mu^0\frac{d\mathbf{e}(\tau)}{d\tau}\,d\tau. \tag{28}$$

Following the same procedure as that of Section 2, the constitutive model of the linear viscoelastic particle-reinforced composites can be then derived, with the similar format to (28) as

$$\bar{\sigma} = \int_0^t \bar{g}_k^0(t-\tau)\bar{k}^0\frac{d\bar{\varepsilon}_m(\tau)}{d\tau}\,d\tau\,\mathbf{I} + 2\int_0^t \bar{g}_\mu^0(t-\tau)\bar{\mu}^0\frac{d\bar{\mathbf{e}}(\tau)}{d\tau}\,d\tau. \tag{29}$$

Here, $\bar{k}^0$ and $\bar{\mu}^0$ are the effective instantaneous bulk and shear moduli, respectively, and the corresponding effective relaxation functions are defined as

$$\begin{aligned}\bar{g}_k^0(t) &= R_v^0 g_k^{0p}(t) + (1-R_v^0)g_k^{0m}(t),\\ \bar{g}_\mu(t) &= R_d^0 g_\mu^{0p}(t) + (1-R_d^0)g_\mu^{0m}(t),\end{aligned} \tag{30}$$

where g_k^{0p}, g_k^{0m}, g_μ^{0p}, and g_μ^{0m} are the relaxation functions of the particles and matrix for the volumetric and deviatoric deformations, respectively. In (30), R_v^0 and R_d^0 are defined as the effective instantaneous strain energy ratios of the particles to composite for the volumetric and deviatoric deformations, respectively. We note that, since both the instantaneous and long-term behaviors are considered to be linearly elastic, $\bar{k}^0$, $\bar{\mu}^0$, R_v^0, and R_d^0 can be thus achieved using the same micromechanical models as those in Section 2.3, through simply replacing the long-term variables by the corresponding instantaneous variables.

To study the full relaxation behaviors of the composites, the classical Maxwell model is employed to characterize the viscoelastic behaviors of the constituents, whose relaxation functions read (Lakes, 2009)

$$g^0(t) = e^{-t/\tau_\alpha}. \tag{31}$$

To verify the prediction accuracy of the constitutive model reformulated with the instantaneous moduli on the full relaxation behaviors of the composites, both the particles and matrix are considered as Maxwellian materials, with the normalized material constants of $E_p = 10$, $\nu_m = 0.25$, $\tau_{\alpha p} = 2$, $E_m = 1$, $\nu_m = 0.35$, and $\tau_{\alpha m} = 1$. Stress relaxations under uniaxial tension are applied to the models with $c = 0.3$. The tensile strains are proportionally applied up to $\varepsilon_{11} = 0.01$ within a normalized time of $t = 1$. Then, the strains are held constant until $t = 5$. The stresses computed from the RVE models and the constitutive model of (29) are presented against the loading time in Fig. 11. As expected, the stresses asymptotically diminish to approach zero with increasing time. During the proportionally loading process, the theoretical prediction coincides well with the FEM results, and the relative difference is only 1.1% at $t = 1$. For the relaxation process, the constitutive model tends to slightly overestimate the FEM results with increasing time. The findings reveal that the constitutive model reformulated can offer sufficiently good predictions on the effective viscoelastic behaviors of the particle-reinforced composites consisting of the Maxwellian constituents.

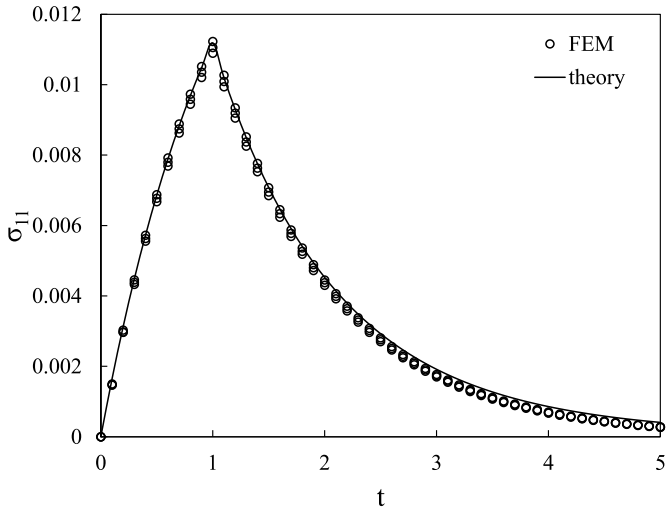

Fig. 11. A comparison between the stresses computed with the constitutive model (lines) and the FEM simulations (symbols) for the particle-reinforced composites consisting of two Maxwellian constituents undergoing relaxations.

6. Concluding remarks

A new homogenization method in the time domain is proposed to decompose the effective responses of linear viscoelastic particle-reinforced composites in terms of the corresponding matrix and particle contributions. The constitutive model is developed by deriving the stresses of the two individual composite constituents and then superposing them. The resulting constitutive formulation has the same form as that of each individual constituent, which offers great advantages on the analysis of the effective mechanical behaviors of viscoelastic particle-reinforced composites in both time and frequency domains.

Representative volume element models of the composite microstructure with different particle volume fractions (i.e., $c = 0.1$, 0.2 and 0.3) are constructed to validate the constitutive model numerically. The effects of the particle volume fraction, the strain rate, the elastic and viscous parameters on the effective viscoelastic behaviors of the composites and the creep behaviors have been comprehensively investigated. The numerical results show that the proposed composite viscoelastic constitutive model can accurately predict the effective properties of linear viscoelastic particle-reinforced composites in the time domain.

The experimental results of the PET reinforced with 15 vol% and 27 vol% glass beads are utilized to validate the proposed constitutive model in the frequency domain. The findings show that the proposed model can provide satisfactory estimates for the effective storage and loss shear moduli of the viscoelastic composites under different

frequencies.

The constitutive model is reformulated with the instantaneous moduli to estimate the linear viscoelastic particle-reinforced composites, whose mechanical behaviors will be fully relaxed. The FEM simulations under relaxations are carried out to validate the constitutive model reformulated. The results reveal that the constitutive model can predicts well the effective behaviors of the composites consisting of the Maxwellian constituents.

Declaration of Competing Interest

The authors declare that we have no conflicts of interest to this work.

Acknowledgements

The financial support from the National Natural Science Foundation of China (Nos. 11572020, 11802007, and 11872162) is greatly appreciated.

References

Azoti, W.L., Bonfoh, N., Koutsawa, Y., Belouettar, S., Lipinski, P., 2013. Influence of auxeticity of reinforcements on the overall properties of viscoelastic composite materials. Mech. Mater. 61, 28–38.
Benveniste, Y., 1987. A new approach to the application of Mori-Tanaka theory in composite-materials. Mech. Mater. 6, 147–157.
Berbenni, S., Dinzart, F., Sabar, H., 2015. A new internal variables homogenization scheme for linear viscoelastic materials based on an exact Eshelby interaction law. Mech. Mater. 81, 110–124.
Brenner, R., Masson, R., Castelnau, O., Zaoui, A., 2002. A “quasi-elastic” affine formulation for the homogenised behaviour of nonlinear viscoelastic polycrystals and composites. Eur. J. Mech. A. Solids 21, 943–960.
Brinson, L.C., Lin, W.S., 1998. Comparison of micromechanics methods for effective properties of multiphase viscoelastic composites. Compos. Struct. 41, 353–367.
Christensen, R.M., 1969. Viscoelastic properties of heterogeneous media. J. Mech. Phys. Solids 17, 23–41.
Christensen, R.M., 1979. Mechanics of Composite Materials. Wiley, New York.
Christensen, R.M., Lo, K.H., 1979. Solutions for effective shear properties in three phase sphere and cylinder models. J. Mech. Phys. Solids 27, 315–330.
Cruz, C., Diani, J., Regnier, G., 2009. Micromechanical modelling of the viscoelastic behaviour of an amorphous poly(ethylene)terephthalate (PET) reinforced by spherical glass beads. Compos. Part A-Appl. Sci. Manufact. 40, 695–701.
DeBotton, G., Tevet-Deree, L., 2004. The response of a fiber-reinforced composite with a viscoelastic matrix phase. J. Compos. Mater. 38, 1255–1277.
Dunn, M.L., 1995. Viscoelastic damping of particle and fiber reinforced composite materials. J. Acoust. Soc. Am. 98, 3360–3374.
Guo, Z., Shi, X., Chen, Y., Chen, H., Peng, X., Harrison, P., 2014. Mechanical modeling of incompressible particle-reinforced neo-Hookean composites based on numerical homogenization. Mech. Mater. 70, 1–17.
Hashin, Z., 1965. Viscoelastic behavior of heterogeneous media. J. Appl. Mech. 32, 630–636.
Hashin, Z., 1970. Complex moduli of viscoelastic composites—I. General theory and application to particulate composites. Int. J. Solids Struct. 6, 539–552.
Hill, R., 1972. Constitutive macro-variables for heterogeneous solids at finite strain. Proc. R. Soc. Lond. Series A-Math. Phys. Sci. 326, 131–147.
Lahellec, N., Suquet, P., 2007a. Effective behavior of linear viscoelastic composites: a time-integration approach. Int. J. Solids Struct. 44, 507–529.
Lahellec, N., Suquet, P., 2007b. On the effective behavior of nonlinear inelastic composites: I. Incremental variational principles. J. Mech. Phys. Solids 55, 1932–1963.
Lakes, R., 2009. Viscoelastic Materials. Cambridge University Press.
Laws, N., McLaughlin, R., 1978. Self-consistent estimates for the viscoelastic creep compliances of composite materials. Proc. R. Soc. Lond. A. Math. Phys. Sci. 359, 251–273.
Li, J., Weng, G.J., 1994. Strain-rate sensitivity, relaxation behavior, and complex moduli of a class of isotropic viscoelastic composites. J. Eng. Mater. Technol. 116, 495–504.
Molinari, A., Ahzi, S., Kouddane, R., 1997. On the self-consistent modeling of elastic-plastic behavior of polycrystals. Mech. Mater. 26, 43–62.
Paquin, A., Sabar, H., Berveiller, M., 1999. Integral formulation and self-consistent modelling of elastoviscoplastic behavior of heterogeneous materials. Arch. Appl. Mech. 69, 14–35.
Ricaud, J.-M., Masson, R., 2009. Effective properties of linear viscoelastic heterogeneous media: internal variables formulation and extension to ageing behaviours. Int. J. Solids Struct. 46, 1599–1606.
Rougier, Y., Stolz, C., Zaoui, A., 1993. Représentation spectrale en viscoélasticité linéaire des matériaux hétérogènes. Comptes Rendus de l'Academie des Sciences Serie II 316, 1517–1522.
Seck, M.E.B., Gărăjeu, M., Masson, R., 2018. Exact solutions for the effective nonlinear viscoelastic (or elasto-viscoplastic) behaviour of particulate composites under isotropic loading. Eur. J. Mech. A. Solids 72, 223–234.
Segurado, J., Llorca, J., 2002. A numerical approximation to the elastic properties of sphere-reinforced composites. J. Mech. Phys. Solids 50, 2107–2121.
Tressou, B., Vaziri, R., Nadot-Martin, C., 2018. Application of the incremental variational approach (EIV model) to the linear viscoelastic homogenization of different types of microstructures: long fiber-, particle-reinforced and strand-based composites. Eur. J. Mech. A-Solids 68, 104–116.
Yi, Y.-M., Park, S.-H., Youn, S.-K., 1998. Asymptotic homogenization of viscoelastic composites with periodic microstructures. Int. J. Solids Struct. 35, 2039–2055.